THE JOURNAL OF BIOLOGICAL CHEMISTRY VOL. 288, NO. 52, pp. 37267–37276, December 27, 2013

Biosynthesis and Expression of a Disintegrin-like and Metalloproteinase Domain with Thrombospondin-1 Repeats-15

*A NOVEL VERSICAN-CLEAVING PROTEOGLYCANASE**

Received for publication, September 10, 2012, and in revised form, November 6, 2013 Published, JBC Papers in Press, November 12, 2013, DOI 10.1074/jbc.M112.418624

Carolyn M. Dancevic[1,2], Fiona W. Fraser[1], Adam D. Smith, Nicole Stupka[3], Alister C. Ward, and Daniel R. McCulloch[4]

From the School of Medicine, Faculty of Health, and Molecular and Medical Research SRC, Deakin University, 75 Pigdons Road, Waurn Ponds, Victoria 3216, Australia

Background: ADAMTS proteoglycanases show proteolytic activity toward versican and other proteoglycans.
Results: ADAMTS15, which cleaves versican, is expressed during early cardiac development and during musculoskeletal development.
Conclusion: With unique and overlapping biological properties, ADAMTS15 is likely to have cooperative roles with other members of the ADAMTS proteoglycanase clade.
Significance: Versican cleavage has profound effects on developmental morphogenesis and regulates cancer cell behavior.

The proteoglycanase clade of the ADAMTS superfamily shows preferred proteolytic activity toward the hyalectan/lectican proteoglycans as follows: aggrecan, brevican, neurocan, and versican. ADAMTS15, a member of this clade, was recently identified as a putative tumor suppressor gene in colorectal and breast cancer. However, its biosynthesis, substrate specificity, and tissue expression are poorly described. Therefore, we undertook a detailed study of this proteinase and its expression. We report propeptide processing of the ADAMTS15 zymogen by furin activity, identifying $RAKR^{212}\downarrow$ as a major furin cleavage site within the prodomain. ADAMTS15 was localized on the cell surface, activated extracellularly, and required propeptide processing before cleaving V1 versican at position $^{441}E\downarrow A^{442}$. In the mouse embryo, *Adamts15* was expressed in the developing heart at E10.5 and E11.5 days post-coitum and in the musculoskeletal system from E13.5 to E15.5 days post-coitum, where it was co-localized with hyaluronan. *Adamts15* was also highly expressed in several structures within the adult mouse colon. Our findings show overlapping sites of *Adamts15* expression with other members of ADAMTS proteoglycanases during embryonic development, suggesting possible cooperative roles during embryogenesis, consistent with other ADAMTS proteoglycanase combinatorial knock-out mouse models. Collectively, these data suggest a role for ADAMTS15 in a wide range of biological processes that are potentially mediated through the processing of versican.

The A disintegrin-like and metalloproteinase domain with thrombospondin-1 repeats (ADAMTS)[5] family includes 19 evolutionarily conserved extracellular matrix (ECM) enzymes in mammals with diverse biological functions according to their substrate specificity (1). In humans, mutations in *ADAMTS13* cause thrombocytopenic purpura (2) in *ADAMTS10* recessive Weil-Marchesani syndrome (3) and in *ADAMTS2* Ehlers-Danlos syndrome type VIIC (4). The proteoglycanase clade of ADAMTS enzymes is an evolutionarily distinct subset of the larger ADAMTS family of which the activity of ADAMTS1, -4, -5, and -9 toward several hyalectans has been characterized. It has been previously shown that ADAMTS1, -4, -5, and -9 direct their catalytic activity toward the $E^{441}\downarrow A^{442}$ bond within the glycosaminoglycan-β domain of versican (V1 splice variant) (5–7). Another member of this family that has the potential to cleave hyalectans is ADAMTS15.

The biosynthesis, activation, and substrate specificity of ADAMTS1, -4, -5, and -9 are well characterized (5, 6, 8–11). In each case, propeptide processing is mediated by paired basic amino acid cleaving enzyme activity, including furin, PACE-4, and PC7. With the exception of ADAMTS9, their propeptide processing initiates catalytic activity toward their preferred substrates, whereas the ADAMTS9 zymogen is constitutively active (12). Relatively little is known regarding the propeptide processing or substrate specificity of ADAMTS15.

Several biological roles for ADAMTS proteoglycanases have been defined using mouse models. *Adamts1* knock-out mice have significantly reduced fertility due to impaired folliculogenesis and ovulation (13) and urinary tract anomalies (14). Homozygous *Adamts9* knock-out mice are embryonic lethal, dying around the time of gastrulation, with palatal shelf mesenchyme proliferation and melanoblast survival/colonization

* This work was supported in part by Financial Markets Foundation for Children Grant 162-10 (to D. McC., N. S., and A. W.) and the Deakin University Faculty of Health, Faculty Development Research Grant FDRG-2009 (to D. McC.).
[1] Both authors contributed equally to this work.
[2] Supported by a Commonwealth Government-funded Australian postgraduate award.
[3] Supported in part by a National Health and Medical Research Council Peter Doherty Fellowship.
[4] To whom correspondence should be addressed: School of Medicine, Faculty of Health, Deakin University, 75 Pigdons Road, Waurn Ponds, VIC 3216, Australia. Tel.: 61-3-5227-2838; Fax: 61-3-5227-2615; E-mail: daniel.mcculloch@deakin.edu.au.

[5] The abbreviations used are: ADAMTS, a disintegrin-like and metalloproteinase domain with thrombospondin-1 repeat; dpc, days post-coitus; BisTris, 2-[bis(2-hydroxyethyl)amino]-2-(hydroxymethyl)propane-1,3-diol; dec, decanoyl; cmk, chloromethyl ketone; PNGaseF, peptide:*N*-glycosidase F; dpc, days post-coitum; CL, cell lysate; CM, conditioned medium.

impaired when one allele of *Adamts9* is removed on an *Adamts20* (belted, *bt*) knock-out mouse background (15, 16). Interdigital apoptosis is compromised in *Adamts5, Adamts9,* and *Adamts20* combinatorial knock-out mice during embryogenesis, and an ADAMTS proteoglycanase generated versican (V1) cleavage product spanning from G1-DPEAAE^{441} is required for BMP-mediated apoptosis to sculpt the developing autopod (17). Homozygous *Adamts5* knock-out mice also present with abnormal heart valves (18, 19). The absence of versican (V0/V1) processing at the defective site during embryonic development of respective *Adamts* proteoglycanase knock-out mice is a common precursor to each phenotype. In contrast, the inactivation of *Adamts5* confers protection against experimentally induced arthritis in the mouse through an apparent lack of aggrecan cleavage in synovial joints (20, 21), making ADAMTS5 a major drug target for arthritis intervention.

ADAMTS15 has recently emerged as a putative tumor suppressor gene (22, 23), because it is functionally inactivated through specific mutations in its gene sequence in colorectal cancer and methylation-induced silencing in breast cancer, where its level of expression is a positive predictor of breast cancer patient survival outcome. In addition, aberrant expression of *ADAMTS15*, along with versican (*VCAN*), is implicated in prostate cancer progression (24, 25), whereas the accumulation of versican in breast, prostate, and ovarian tumors can promote metastasis (26–28).

Despite the putative tumor-suppressor role of *ADAMTS15* in several cancers, little is known about its basic biology and biochemistry. Therefore, we have investigated its biosynthesis, mechanism of activation, localization, activity toward versican, and expression pattern. We show that the propeptide processing of ADAMTS15 by furin activity is a requirement for versican processing, thus demonstrating for the first time that ADAMTS15 is a versicanase. We further describe the expression and localization of ADAMTS15 in key sites of the developing mouse embryo that overlap with other ADAMTS proteoglycanases and versican, as well as demonstrate the expression of ADAMTS15 in the adult mouse colon. These data provide insight into potential functional overlap with other versican-degrading ADAMTS enzymes.

EXPERIMENTAL PROCEDURES

Generation of Adamts15 Constructs —Mouse full-length *Adamts15* cDNA was purchased from Origene Technologies (Rockville, MD), and the following primers were used to amplify full-length *Adamts15*: forward 5′-atccgaattcacc*atgcttctgctg*-3′ and reverse 5′-gcat**gcggccgc**tt*gcagggtctcaa*-3′, where boldface indicates EcoRI and NotI restriction digest sites, respectively; italics indicate gene-specific sequence, and underlines indicate Kozak sequence. After the amplification and restriction digest, the coding sequence was ligated into pcDNA3.1MycHisA+ (Invitrogen). To generate deletion constructs, the T7 priming site present in pcDNA3.1MycHisA+ was utilized as a common forward primer in combination with the following reverse primers: *Adamts15*-II, 5′-gcat**gcggccgc**ttgggctggtccag-3′; *Adamts15*-III, 5′-ggat**gcggccgc**ttcacccggtactt-3′; *Adamts15*-IV, 5′-ggat**gcggccgc**ttggggcagggctc-3′; *Adamts15*-V, 5′-ggat**gcggccgc**ttcactacaaaatt-3′; *Adamts15*-VI, 5′-ggat**gcggccgc**tttctgttatctgg-3′; and *Adamts15*-VII, 5′-ggat**gcggccgc**tttgggcagggttc-3′, where boldface indicates NotI restriction sites, and underlines indicate gene-specific sequences. The resultant PCR products were digested and cloned into pcDNA3.1MycHisA+ as described above. Site-directed mutagenesis was performed using the QuikChange Lightning site-directed mutagenesis kit (Agilent Technologies, Blackburn, Australia) with the following primers: R212A forward, 5′-gtctgggcgcgccaagGCcttcgtgtctataccacg-3′, and reverse, 5′-cgtggtatagacacgaagGCcttggcgcgcccagac-3′; E362A forward, 5′-ttcaccactgcccatgCgctgggccatgtgttc-3′, and reverse 5′-gaacacatggcccagcGcatgggcagtggtgaa-3′; N141Q forward, 5′-tcattagccctctgcccCaAaccagcgcgccagag-3′, and reverse, 5′-ctctggcgcgctggtTtGgggcagagggctaatga-3′ (where capital letters indicate base mutations). All newly generated construct cDNAs were confirmed by Sanger direct DNA sequencing (Australian Genome Research Facility, Melbourne, Australia) using vector-specific primers and the following gene-specific sequencing primers: 436F, 5′-gaggcgcagcgtcacagc-3′, and 739R, 5′-cagcagcgtcagtagata-3′; 970F, 5′-gctaccacctgtgacac-3′, and 1226R, 5′-gtcagcctgcagcgctgc-3′ (numbers indicate base positions corresponding to GenBank^{TM} accession number NM_001024139.1).

Cell Culture and Transfection—HEK293T and COS-7 cells (ATCC, Manassas, VA) were grown in Dulbecco's modified Eagle's medium (DMEM) containing 10% fetal bovine serum (FBS) (Invitrogen) in an atmosphere of 5% CO_2 at 37 °C in a CO_2 incubator (HERAcell 150i, Thermo Scientific, Scoresby, Australia). Cells were seeded at 4×10^5 cells per well in 6-well plates (Corning Life Sciences, Mount Martha, Australia). Constructs encoding full-length *Adamts15*, its respective deletions or site-directed mutants, full-length *ADAMTS5* (6), ProCat ADAMTS9 (5), or a full-length V1 versican construct (kindly provided by Professor Dieter Zimmerman) were added to serum-free DMEM containing Lipofectamine-2000 (Invitrogen). The Lipofectamine/DNA (1 or 2 μg/well) complex was added to each well in 2 ml of growth medium. After 4–5 h of incubation, growth medium was removed, and 1 ml of serum-free DMEM per well was added to the cells. Forty eight hours later, the conditioned media (CM) was collected, and cells were harvested in ice-cold PBS with a cell scraper from which cell lysate (CL) was extracted using 1% Triton X-100 in 150 mM NaCl, 20 mM Tris-HCl, pH 7.5, containing EDTA-free complete protease inhibitor mixture (Roche Applied Science). Resultant CM and CL samples were stored at −80 °C until further processing.

Western Blotting—Standard Western blotting procedures were used to analyze recombinant ADAMTS15 protein following the above transfections with or without the synthetic furin inhibitor decanoyl-Arg-Val-Lys-Arg-chloromethyl ketone (dec-RVKR-cmk) (Enzo LifeSciences, Exeter, UK), heparin sodium salt (Sigma), or PNGaseF (New England Biolabs, Ipswich, ME) treatment. Protein samples were typically run on 6, 7.5, or 10% BisTris acrylamide gels (Bio-Rad) and separated by SDS-PAGE under reducing conditions alongside the Precision Plus protein standard (Bio-Rad). After transfer to PVDF membrane (LICOR Biosciences), nonspecific sites were blocked with 5% skim milk in TBS-T (150 mM NaCl, 20 mM Tris-HCl, pH 7.5, 0.1% Tween 20) or Odyssey blocking buffer (LICOR Biosci-

ences). Anti-Myc clone 9E3 (Sigma) or anti-ADAMTS15 propeptide (catalog no. Ab45047, Abcam) antibodies were typically used at 1:5000 to detect recombinant proteins in CL and CM. The anti-V0V1 (catalog no. PA1-1748A, Thermo Scientific) antibody (1:500) was used to detect cleaved versican (DPEAAE epitope), and anti-glycosaminoglycan-β (catalog no. AB1033, Merck) antibody (1:5000) was used to detect full-length V1 versican. Anti-GAPDH (Merck) was used to assess levels of loading as described previously in both CL and CM (29, 30). Primary antibodies were incubated overnight at 4 °C followed by TBS-T washes. Secondary antibodies (anti-rabbit IR800 (Sapphire Bioscience) or anti-mouse IR680 (Sigma)) were incubated for 1 h at room temperature, followed by TBS-T washes. The Odyssey (LICOR) imaging system was used to detect 800 nm (green) and 700 nm (red) IR antibodies. Typical settings included the following: resolution 169 μm, medium quality, 3.0-mm focus offset, and an intensity level of 5 for each 700- and 800-nm scans. Most Western blots were detected using chemiluminescence; in these cases, the same procedure was followed except the secondary antibodies (goat anti-rabbit or goat anti-mouse) were conjugated with horseradish peroxidase (Dako, Australia), and the signal was detected on film (Eastman Kodak) using ECL or ECL-prime (GE Healthcare).

Cell-surface Biotinylation—Cell-surface biotinylation was performed as described previously for the detection of ADAMTS9 ProCat on the cell surface (5). Briefly, COS-7 cells transfected with full-length ADAMTS15 (ADAMTS15-I), ADAMTS15 ProCat (ADAMTS15-VII), or ADAMTS9 ProCat (positive control) (5) were harvested and treated with or without trypsin before biotinylation. Biotinylated proteins were captured with streptavidin-agarose (Sigma) and eluted by boiling in Laemmli sample buffer. The anti-Myc antibody was used on subsequent Western blots to detect Myc-tagged full-length ADAMTS15 (ADAMTS15-I), ADAMTS15 ProCat (ADAMTS15-VII), or ADAMTS9 ProCat. Untransfected cells were included in the procedure as a negative control.

Versicanase Assays —Versicanase assays were performed essentially as described previously (6, 12, 17, 29). Briefly, 50 μl of CM was combined with 50 μl of CM containing versican (V1 splice variant) and incubated at 37 °C for 16 h. After boiling and incubation on ice, 5 milliunits of chondroitinase ABC (Seikagaku, Tokyo, Japan) per reaction was added to the samples and incubated for 2 h at 37 °C to ensure glycosaminoglycan chains were cleaved for effective resolution of the core protein by SDS-PAGE as described above.

Generation of Mouse Embryos—The Deakin University Animal Welfare Committee approved all experiments performed on animals in accordance with the National Health and Medical Research Council guidelines for care and use of animals in research. Timed overnight matings between 6- and 8-week-old C57/Bl6J mice (Animal Resource Centre, Perth, Australia) were confirmed by the observation of a vaginal plug before 0900 h the following morning, at which time the embryonic age was designated as E0.5 days post-coitum (dpc). Mice were humanely killed in a CO_2 chamber as per the Deakin University Animal Welfare Committee approved standard operating procedures, and the embryos harvested for further processing.

In Situ Hybridization—*In situ* hybridization was performed essentially as described previously (17, 31). Briefly, harvested embryos were fixed overnight in 4% paraformaldehyde in PBS at 4 °C, dehydrated through a series of methanol (MeOH)/PBS/Tween (1%) washes to 100% MeOH, and stored at −80 °C until *in situ* hybridization was performed. Constructs (pGemTeasy, Promega) containing cDNA that was amplified from distinct regions of mouse *Adamts15* cDNA with the following primers sets: probe 1, mTS15_4301F, 5′-tggctttcctgatcccatag-3′, and mTS15_4708R, 5′-gctctaggggctaagctggt-3′; and probe 2, mTS15_4583F, 5′-cagcggaggactagatggag-3′, and mTS15_5007R, 5′-atgcccttcacccactgtag-3′ (numbers indicate base positions corresponding to GenBank™ accession number NM_001024139.1) were linearized by restriction digest. For generation of digoxigenin-labeled sense and antisense cRNA probes, a digoxigenin-labeling kit from Roche Applied Science with either SP6 or T7 RNA polymerases was utilized. Hybridization was performed overnight at 68 °C followed by a series of stringent washes in SDS and sodium citrate/sodium chloride (SSC, pH 7). Detection was facilitated by an overnight incubation with an anti-digoxigenin alkaline phosphate antibody followed by 24 h of washing in TBS-T (1%). 5-Bromo-4-chloro-3-indolyl phosphate/nitro blue tetrazolium (Roche Applied Science) was used as a substrate for detection. Bright field whole-mount images were acquired on an Olympus SZX12 stereomicroscope.

Immunofluorescence—Immunofluorescence was performed essentially as described previously (17, 32) on paraformaldehyde-fixed paraffin-embedded sections (5 μM) with the same anti-ADAMTS15 propeptide antibody described above for Western blotting (1:1000). Alexa fluor FITC-conjugated or Alexa fluor 597-conjugated goat anti-rabbit immunoglobulin (Molecular Probes) was used as the secondary antibody. For co-localization with hyaluronan, biotinylated hyaluronan-binding protein (a kind gift from Associate Professor Amanda Fosang) was used in conjunction with streptavidin-FITC (Sigma) for detection. The immunogenic peptide (catalog no. Ab45243, Abcam) corresponding to the anti-ADAMTS15 epitope was used as a blocking control. In all cases, normal goat serum (Dako) was used to block nonspecific antigen-binding sites prior to incubation with the primary antibody. Nuclei were counterstained and slides mounted with Vectashield-DAPI mounting medium (Vector Laboratories, Burlingame, CA). Antigen retrieval was not necessary. Images were obtained on an automated confocal microscope (Fluoview FV10i, Olympus) using FITC (excitation 495 nm/emission 519 nm) or Alexa Red (excitation 590 nm/emission 618 nm) alongside the DAPI channel (excitation 359 nm/emission 451 nm) to visualize the nuclei. The manufacturer's default imaging software package (Fluoview V2.1B) was used for image analyses. Adobe Photoshop version CS6 software was used to construct the corresponding immunofluorescence images.

RESULTS

Expression of Adamts15 Deletion Constructs in HEK293T and COS-7 Cells—To examine the biosynthesis, activation, and substrate recognition of ADAMTS15, we generated constructs encoding C-terminally Myc/His-tagged mouse ADAMTS15

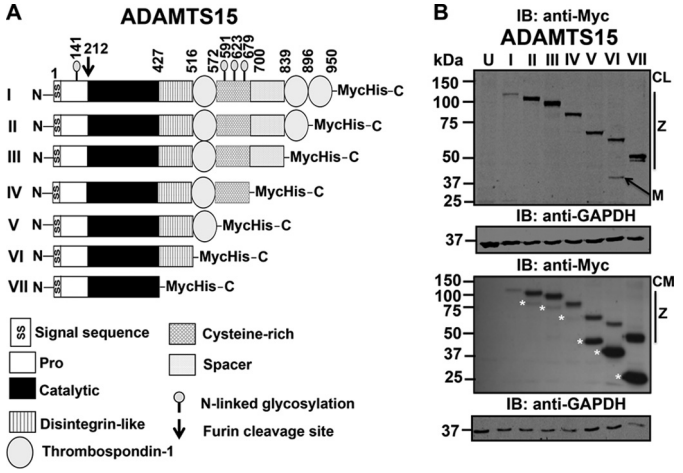

FIGURE 1. **ADAMTS15 expression constructs and their expression.** *A*, schematic diagram of full-length (*I*) and truncated (*II–VII*) forms of ADAMTS15. Functional domains and sequences are shown, with relevant amino acids *numbered*. The furin cleavage site present in the prodomain is represented with an *arrow*, and the C-terminal Myc/His tag indicated. *B*, expression of full-length ADAMTS15 (ADAMTS15-I) and its domain deletion constructs (*ADAMTS15-II–VII*) in COS-7 CL (*top panel*) and the corresponding CM (*3rd panel, asterisks* indicate mature forms of ADAMTS15) using the anti-Myc antibody. GAPDH was used as a loading control in both CL (*2nd panel*) and CM (*bottom panel*). Only the mature form of ADAMTS15-VI was detected in the CL. Note the increasingly poor detection of ADAMTS15-I through IV in the CM. Similar results were obtained in transfected HEK293T cells. *Z,* zymogen; *M,* mature; *U,* untransfected; *IB,* immunoblot.

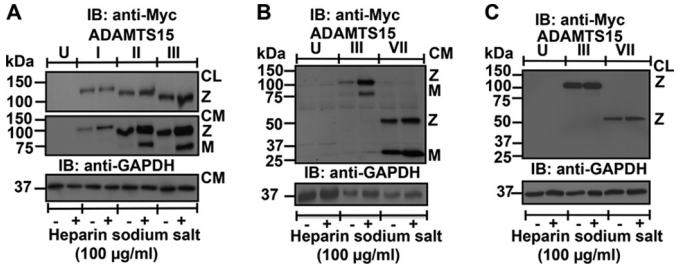

FIGURE 2. **ADAMTS15 detection is enhanced by the addition of heparin.** *A*, expression of full-length ADAMTS15 (ADAMTS15-I), deletion constructs ADAMTS15-II and ADAMTS15-III in CL (*top panel*), and the corresponding conditioned media (*CM*) (*middle panel*) ± heparin sodium salt treatment using the anti-Myc antibody. GAPDH was used as a loading control in CM (*bottom panel*). Note the enhanced detection of each form of ADAMTS15 in CM with the addition of heparin. *B*, expression of ADAMTS15-III (positive control) and ADAMTS15 ProCat (ADAMTS15-VII) in CM ± heparin sodium salt treatment using the anti-Myc antibody (*top panel*). GAPDH was used as a loading control in CM (*bottom panel*). A small but consistent enhancement in detection of ProCat was seen in CM upon heparin treatment. *C*, expression of ADAMTS15-III (positive control) and ADAMTS15 ProCat (ADAMTS15-VII) in CL (*top panel*) corresponding to the CM shown in *B*, detected with the anti-Myc antibody. GAPDH was used as a loading control in CL (*bottom panel*). *Z,* zymogen; *M,* mature; *U,* untransfected; *IB,* immunoblot.

(Fig. 1*A*) and expressed them as recombinant proteins in both HEK293F and COS-7 cells. The resultant CL and CM were analyzed by Western blot. All constructs were efficiently detected in cell lysates of HEK293T cells and COS-7 cells. Using the anti-Myc antibody, full-length ADAMTS15 and each deletion mutant appeared at the predicted molecular weight of the zymogen in the CL (Fig. 1*B, top panel*). GAPDH was used a loading control in CL (Fig. 1*B, 2nd panel*). In the corresponding CM, deletion mutants ADAMTS15-V, -VI, and VII robustly appeared at both the predicted molecular weights of the zymogen and corresponding mature proteins, indicating the propeptide had been proteolytically processed extracellularly (Fig. 1*B, 3rd panel*; *asterisks* indicate mature proteins). GAPDH was used as loading control for CM (Fig. 1*B, bottom panel*). Mature forms of full-length ADAMTS15 and the remaining deletion mutants were less apparent despite additional attempts to concentrate the medium (data not shown), although subsequent Western blots using ECL prime and long exposure times facilitated their detection (see below).

Next, we added serum-free media ± heparin sodium salt post-transfection for 48 h, prior to harvesting the cells. Fig. 2*A* shows robust expression of zymogens for full-length ADAMTS15 (ADAMTS15-I), ADAMTS15-II, and -III deletion mutants in the CL (*top panel*). In the CM, detection of both zymogen and mature ADAMTS15-I, ADAMTS15-II, and ADAMTS15-III protein was enhanced by the addition of heparin (Fig. 2*A, middle panel*). ADAMTS5 was used as a positive control (data not shown) as it has been previously reported to be heparin-sensitive (6). These data suggested a strong association of ADAMTS15 with the ECM via putative heparin-binding sites. The GAPDH loading controls are shown for the CM (Fig. 2*A, bottom panel*). In additional experiments, heparin sensitivity was not as apparent for the ADAMTS15-IV deletion mutant (data not shown). We therefore concluded that the spacer domain of ADAMTS15 could mediate heparin binding but could not rule out the possibility that domains C-terminal to the spacer domain also possess heparin-binding properties.

To determine whether ADAMTS15 ProCat (ADAMTS15-VII) was also heparin-sensitive, we repeated the experiment with the ADAMTS15 ProCat construct using ADAMTS15-III as a positive control. Heparin enhanced the detection of both the zymogen and mature forms of ADAMTS15 ProCat (ADAMTS15-VII) in the CM (Fig. 2*B, top panel*), indicating that the catalytic domain of ADAMTS15 could also possess ECM-binding properties. ADAMTS15 ProCat zymogen levels in the corresponding CL were similar between treatments (Fig. 2*C, top panel*). GAPDH was used as a loading control for CM (Fig. 2*B, bottom panel*) and CL (Fig. 2*C, bottom panel*).

Adamts15 Is Cell-surface Localized—To understand whether ADAMTS15 is localized to the cell surface, we performed cell-surface biotinylation on transfected cells as described previously for the related proteoglycanase ADAMTS9 (5). Both full-length (ADAMTS15-I) and ProCat (ADAMTS15-VII) zymogens were present on the cell surface, along with the ADAMTS9 ProCat zymogen, which was used as a positive control (Fig. 3*A, asterisks*) (5). Robust levels of each zymogen were detected in the corresponding CL (Fig. 3*B, top panel*), with GAPDH used as proxy readout of cellular input (Fig. 3*B, bottom panel*).

ADAMTS15 Propeptide Is Cleaved by Furin at Position RAKR^{212}—Because the ADAMTS15 ProCat (ADAMTS15-VII) construct was robustly expressed and processed, we used this construct to determine the mechanism of ADAMTS15 propeptide processing in a similar manner to that previously described for ADAMTS5 and ADAMTS9 (5, 6). Cell lines expressing *Adamts15-VII* were treated with the furin-specific inhibitor dec-RVKR-cmk. The addition of 50 μM dec-RVKR-cmk to transfected cells had no effect on zymogen levels in CL samples (Fig. 4*A, top panel*) but significantly enhanced detection of the

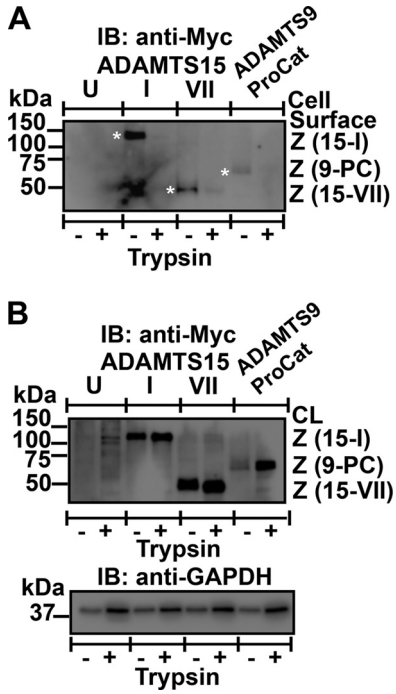

FIGURE 3. **ADAMTS15 is localized to the cell surface.** *A*, full-length ADAMTS15 (ADAMTS15-I), ADAMTS15 ProCat (ADAMTS15-VII), and ADAMTS9 ProCat (positive control) were detected on the cell surface (*asterisks*) with minimal to no detection on trypsin-treated cells. *B,* levels of zymogens detected in CL after cell-surface biotinylation (*top panel*) and corresponding levels of GAPDH (*bottom panel*). *Z,* zymogen; *9-PC,* ADAMTS9 ProCat; *U,* untransfected; *IB,* immunoblot..

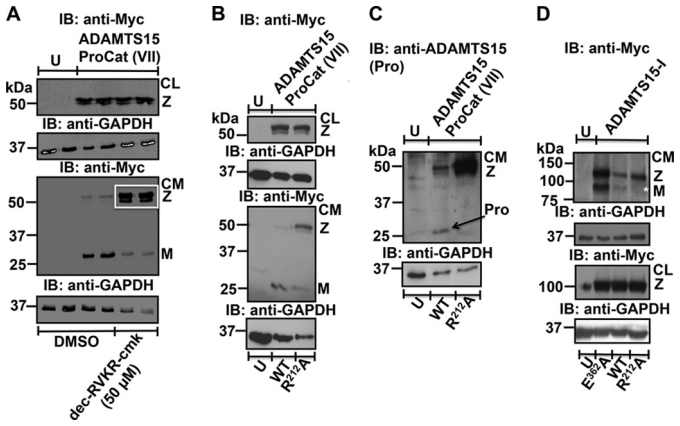

FIGURE 4. **ADAMTS15 propeptide processing.** *A*, expression of ADAMTS15 ProCat (ADAMTS15-VII) treated ± furin inhibitor dec-RVKR-cmk in COS-7 CL (*top panel*) and CM (*3rd panel*) using the anti-Myc antibody. GAPDH was used as a loading control in both CL (*2nd panel*) and CM (*bottom panel*). Note the enhanced detection of the zymogen in the CM upon treatment with the furin inhibitor (*3rd panel, white box*) and corresponding decrease in expression of the mature form. *DMSO,* vehicle control. *B*, expression of ADAMTS15 ProCat (ADAMTS15-VII) and its corresponding R212A mutant in COS-7 CL (*top panel*) and CM (*3rd panel*) using the anti-Myc antibody. GAPDH was used as a loading control in both CL (*2nd panel*) and CM (*bottom panel*). Note the enhanced detection of the R212A mutant zymogen in the CM (*3rd panel*) and corresponding decrease in expression of the mature form. *C*, expression of ADAMTS15 ProCat (ADAMTS15-VII) and its corresponding R212A mutant in COS-7 CM (*top panel*) detected with the anti-ADAMTS15 propeptide antibody. GAPDH was used as a loading control in the CM (*bottom panel*). Note the enhanced detection of the R212A mutant zymogen in the CM and corresponding decrease in detection of the prodomain. *Pro,* prodomain. *D*, expression of full-length ADAMTS15 (ADAMTS15-I) wild type, E362A, and R212A in the CM of transfected COS-7 cells (*top panel*). Similar levels of zymogens were observed in the corresponding CL (*3rd panel*). GAPDH was used as a loading control in both CM (*2nd panel*) and CL (*bottom panel*). *Z,* zymogen; *M,* mature; *U,* untransfected; *WT,* wild type; *IB,* immunoblot.

Myc-tagged zymogen in the CM (Fig. 4*A, 3rd panel, white box*) and reduced the levels of the mature form accordingly, indicating that furin activity was necessary for ADAMTS15 propeptide cleavage. GAPDH was used as a loading control for CL (Fig. 4*A, 2nd panel*) and CM (Fig. 4*A, bottom panel*). We next mutated the P1 arginine residue of the predicted furin cleavage site $RAKR^{212}\downarrow$ to an alanine (R212A) in the ADAMTS15-VII construct and expressed it in HEK293T or COS-7 cells. Similar to the treatment with dec-RVKR-cmk, the R212A mutation led to a reduction of propeptide cleavage in the CM (Fig. 4*B, 3rd panel*) with no effect on levels of zymogens in the CL (Fig. 4*B, top panel*). GAPDH was used as a loading control in CL (Fig. 4*B, 2nd panel*) and CM (Fig. 4*B, bottom panel*). Similar results were seen in CM using the anti-ADAMTS15 propeptide antibody (Fig. 4*C, top panel*) confirming that $RAKR^{212}\downarrow$ is a major furin cleavage site for ADAMTS15 propeptide processing. GAPDH was used as a loading control in CM (Fig. 4*C, bottom panel*). To confirm full-length ADAMTS15 was similarly processed, we introduced the same R212A mutation into the ADAMTS15-I construct and observed that propeptide processing was also reduced compared with either wild type or catalytically inactive (E362A) ADAMTS15 in CM (Fig. 4*D, top panel, asterisk*). However, the effect was less striking, possibly due to the poorer levels of detection of full-length ADAMTS15 as compared with its ProCat counterpart. Similar levels of zymogens were seen in the corresponding CL (Fig. 4*D, 3rd panel*). GAPDH was used as a loading control in CM (Fig. 4*D, 2nd panel*) and CL (Fig. 4*D, bottom panel*).

Pro-domain of ADAMTS15 Is N-Glycosylated—Next, we determined the extent of *N*-glycosylation of ADAMTS15 because it contains four predicted *N*-glycosylation sites (UniProtKB/Swiss-Prot accession number P59384) (Fig. 1*A*). Treatment of full-length ADAMTS15 expressed in COS-7 cells with PNGaseF produced a reproducible increase in its electrophoretic mobility (Fig. 5*A*) indicating the presence of *N*-linked glycosylation. When we treated the ADAMTS15 ProCat protein, also expressed in COS-7 cells, with PNGaseF, the zymogen doublet seen in other experiments (for example Fig. 4, *A* and *B, top panels*) disappeared, and we observed enhanced detection of the lower molecular weight species (Fig. 5*B*). Site-directed mutagenesis of the putative *N*-glycosylation site in the ProCat construct (N141Q) generated a band of equivalent electrophoretic mobilities to the lower band (Fig. 5*C*). Further treatment of N141Q ProCat with PNGaseF had no effect on its electrophoretic mobility (Fig. 5*D*). Thus, the predicted *N*-glycosylation site on the prodomain of ADAMTS15 (Fig. 1*A*) is modified by *N*-linked glycans in this expression system. Notably, the *N*-glycan-deficient ADAMTS15 ProCat zymogen was effectively secreted from the cell into the CM (Fig. 5*E, top panel*), unlike the ADAMTS9 ProCat, which required *N*-glycosylation for effective secretion (12). GAPDH was used as a loading control in CM (Fig. 5*E, bottom panel*).

ADAMTS15 Cleaves V1 Versican at $E^{441}\downarrow A^{442}$ to Generate the G1-DPEAAE Neoepitope—Because ADAMTS15 is phylogenetically related to the proteoglycanase clade of ADAMTS enzymes, it was important to determine whether it too had proteolytic activity toward versican (V1) (Fig. 6*A*), as described

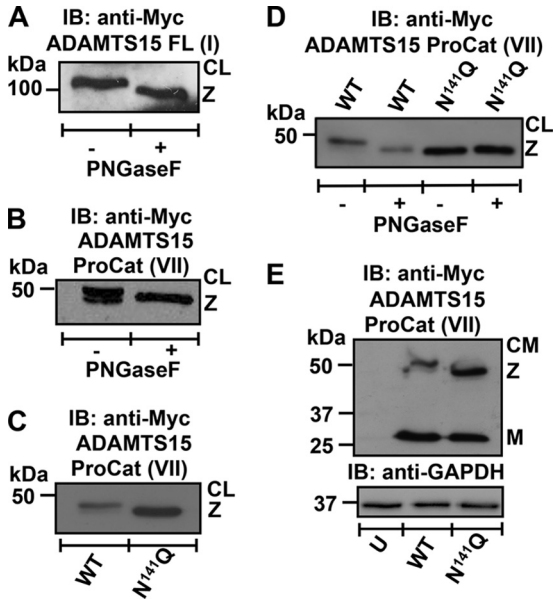

FIGURE 5. **ADAMTS15 is modified by *N*-linked glycans.** *A* and *B*, expression of full-length ADAMTS15 (ADAMTS15-I) and ProCat ADAMTS15 (ADAMTS15-VII), respectively, in transfected COS-7 CL subsequently treated with PNGaseF and detected using the anti-Myc antibody. Note the ProCat doublet in *B* reduced to singlet species upon treatment with PNGaseF. *C*, expression of ADAMTS15 ProCat (ADAMTS15-VII) N141Q in COS-7 cells results in a similar shift in electrophoretic mobility as shown in *B*. *D*, treatment of recombinant wild type or N141Q ADAMTS15 ProCat (ADAMTS15-VII) with PNGaseF. Note that no further electrophoretic mobility shift was observed in the N141Q recombinant ADAMTS15 ProCat (ADAMTS15-VII) protein when treated with PNGaseF. *E*, expression of wild type or N141Q ADAMTS15 ProCat (ADAMTS15-VII) in COS-7 CM (*top panel*). GAPDH was used as a loading control in CM (*bottom panel*). *WT,* wild type; *Z,* zymogen; *M,* mature; *U,* untransfected; *IB*, immunoblot.

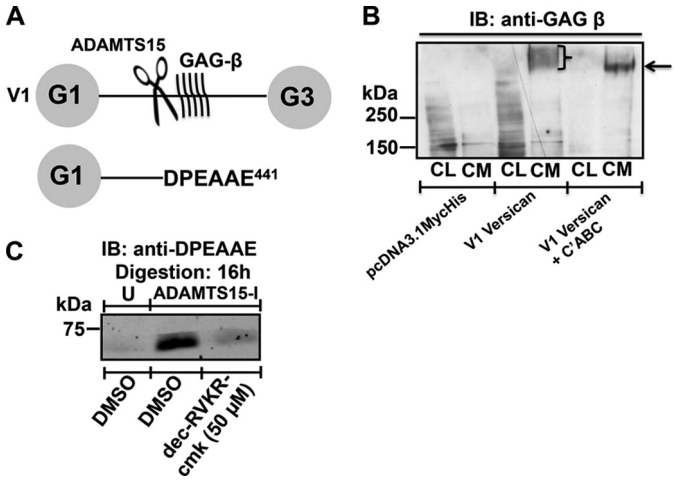

FIGURE 6. **ADAMTS15 cleaves versican at E441A generating the G1-DPEAAE neoepitope.** *A*, schematic representation of V1 versican cleavage by ADAMTS15 generating the DPEAAE neoepitope. *B*, expression of V1 versican in CM of HEK293T cells (*open bracket* and *arrow*). *C' ABC* = chondroitinase ABC. *C*, detection of the DPEAAE neoepitope generated by full-length ADAMTS15 (ADAMTS15-I) after biosynthesis ± dec-RVKR-cmk and subsequent incubation with recombinant V1 versican-enriched conditioned medium represented in *B*. *DMSO,* vehicle control. *U,* untransfected; *GAG*, glycosaminoglycan; *IB*, immunoblot.

previously for several other ADAMTS proteoglycanases. Using recombinant V1 versican-enriched CM (Fig. 6*B*) in a well established assay (6, 12, 17, 29), full-length (ADAMTS15-I) (Fig. 6*C*) showed robust versicanase activity after a 16-h incubation. The addition of dec-RVKR-cmk during its biosynthesis, prior to adding the V1 versican substrate, reduced full-length V1 versicanase activity to background levels (Fig. 6*C*), demonstrating that prodomain removal is necessary for catalytic activation and substrate cleavage by ADAMTS15. In separate versicanase assays, we also observed versican cleavage by ADAMTS15 ProCat (data not shown).

Adamts15 Expression Overlaps with Other ADAMTS Proteoglycanases and Versican in Key Developmental Time Points during Murine Embryogenesis and Is Highly Expressed in the Mouse Colon—Using *in situ* hybridization, alongside immunofluorescence with the ADAMTS15 anti-propeptide antibody used in Fig. 4*C*, we further defined key sites of expression of *Adamts15* during mouse embryogenesis and in the adult colon. Early in development (E10.5 dpc), *Adamts15* mRNA was strongly and specifically expressed in the developing heart tubes (Fig. 7*A, top panels*). By E13.5 dpc, it became widely expressed in sites overlapping with those reported for other members of the ADAMTS proteoglycanases, including the perichondrium in the developing autopod, the brain, ear, whisker follicles, the vertebral column, and the epidermis (Fig. 7*A, middle* and *bottom panels*). The same structures are shown in serial sections as staining positive for *Adamts15* in a C57/Bl6 E14.5 dpc embryo on www.genepaint.org (Set ID: EB1749).

Immunostaining showed ADAMTS15 localization to the myocardium of the developing right atrium, the bulbous cordis (part of the future right ventricle) and in the airway epithelia of the main bronchiole in the lung bud at E11.5 dpc (Fig. 7*B*, *top panel*), the vertebral column and dorsal root ganglia at E14.5 dpc (Fig. 7*B, 2nd panel*), and several sites in the developing hind limb, including the epidermis, joint capsule, patella, and patella-associated tendons and cartilage condensations of developing synovial joints and developing skeletal muscle at E15.5 (Fig. 7*B, 3rd, 4th,* and *bottom panels*). ADAMTS15 and hyaluronan co-localized in several structures within E15.5 developing hind limbs, notably surrounding chondrocytes (Fig. 7*C, top panel*), within developing skeletal muscle and loose mesenchyme (Fig. 7*C, 2nd* and *3rd panels* respectively), and in the epidermis (Fig. 7*C, 4th panel*). In the adult mouse colon, ADAMTS15 was highly expressed in the muscularis externa (inner circular smooth muscle and outer longitudinal smooth muscle), muscularis mucosa, submucosal glands, crypt, and villi epithelial cells, goblet cells, and lamina propria (Fig. 7*D*). Pre-absorption with the immunogenic peptide greatly reduced the signal to background levels (Fig. 7*D, bottom right-hand panel*) indicating the ADAMTS15 antibody was specific to its corresponding ADAMTS15 peptide epitope.

DISCUSSION

The ADAMTS proteoglycanases have emerged as key mediators of several physiological and disease processes (1, 33). Most notable are their roles during embryonic development where they mediate profound morphogenetic processes such as palatal shelf closure and pentameric digit formation (15, 17). In addition, ADAMTS members are also required for normal heart development (18, 19), and neural crest cell-derived pigmentation (16). In most cases, versican proteolysis by the

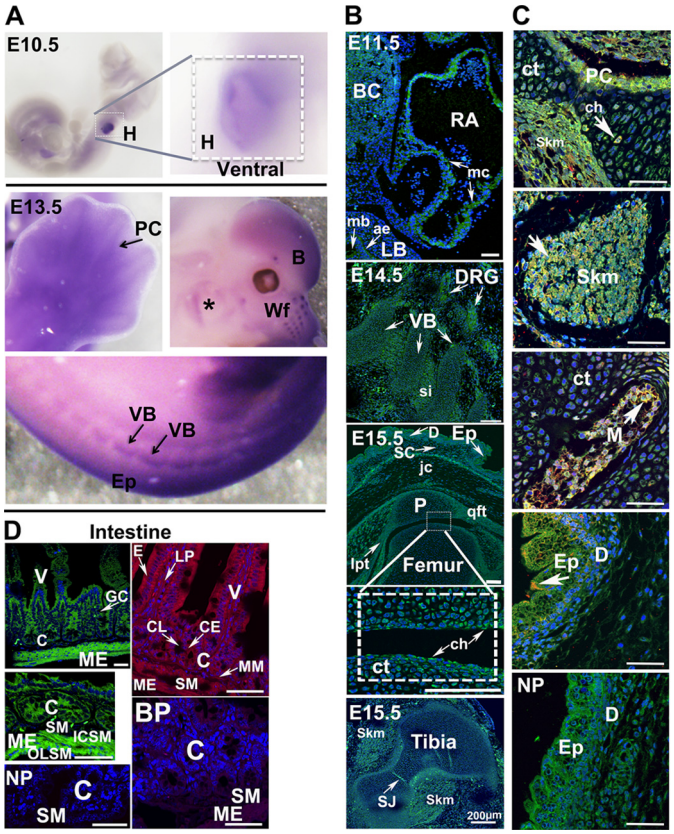

FIGURE 7. **Expression of mouse *Adamts15* during embryogenesis and in the adult colon.** *A*, whole-mount *in situ* hybridization of *Adamts15* in E10.5 (*top panels*) and E13.5 dpc mouse embryos (*middle* and *bottom panels*). *Asterisk, ear*; *B*, brain; *Ep,* epidermis; *H,* heart; *PC,* perichondrium; *VB,* vertebrae; *Wf,* whisker follicles. Similar results were seen with two probes targeted to *Adamts15* mRNA. *B*, immunohistochemistry using the anti-ADAMTS15 propeptide antibody in sections from E11.5, E14.5, and E15.5 dpc mouse embryos. For E11.5: *BC,* bulbous cordis; *RA,* right atrium; *mc,* myocardium; *LB,* lung bud; *mb,* main bronchiole; *ae,* airway epithelia. For E14.5: *DRG,* dorsal root ganglia; *VB,* vertebrae; *si,* segmental interzone. For E15.5: *Ep,* epidermis; *D,* dermis; *SC,* subcutis; *jc,* joint capsule; *p,* cartilage primordium of patella; *lpt,* ligamentum patellae; *qft,* quadriceps femoris tendon; *white inset*: *ct,* cartilage condensations; *ch,* chondrocytes; *SJ,* synovial joint; *Skm,* skeletal muscle. *Scale bars,* 50 μm except where indicated. *C,* immunohistochemistry using the anti-ADAMTS15 propeptide antibody (*red*) and biotinylated hyaluronan-binding protein (*green*) in sections from E15.5 dpc mouse embryos. Co-localization (*arrows*) = *yellow*. *ct,* cartilage condensations; *ch,* chondrocytes; *Skm,* skeletal muscle; *PC,* perichondrium; *M,* mesenchyme; *D,* dermis; *Ep,* epidermis; *NP,* no primary antibody control. *Scale bars,* 50 μm. *D*, immunohistochemistry using the anti-ADAMTS15 propeptide antibody in sections from an adult mouse intestine. *ME,* muscularis externa; *V,* villi; *SM,* submucosa; *GC,* goblet cell; *C,* crypts; *CL,* crypt lumen; *CE,* crypt epithelia; *E,* epitheium of villi; *LP,* lamina propria; *MM,* muscularis mucosa; *ICSM,* inner circular smooth muscle; *OLSM,* outer longitudinal smooth muscle; *NP,* no primary antibody; *BP,* blocking peptide (pre-absorption control). *Scale bars,* 50 μm. *B*, *C*, and *D*, *blue* indicates DAPI-stained nuclei.

ADAMTS proteoglycanases precedes normal development, suggesting this to be a key mediator of those processes.

ADAMTS15 has recently taken the spotlight as a putative tumor suppressor gene in breast and colon cancer (22, 23). In addition, along with versican, it is also dysregulated in prostate cancer (24, 25). To our knowledge, however, a knock-out mouse model for *Adamts15* is currently unavailable, and its biology is poorly described. As a highly conserved member of the proteoglycanase family, ADAMTS15 represents a putative versicanase. In this study, we have characterized the biosynthesis of ADAMTS15, determined its mechanism of activation and extracellular localization, and confirmed its activity toward V1 versican. We have also delineated its expression in key structures of the developing mouse embryo and the adult mouse colon.

The ADAMTS15 zymogen is processed extracellularly, similar to ADAMTS5 and ADAMTS9 (5, 6), and in contrast to ADAMTS1 and ADAMTS4, which are both activated intracellularly (8, 10, 34). The mechanism protecting intracellular propeptide processing of a select subset of the ADAMTS proteoglycanases is currently unknown. However, knowing their site(s) of activation is important when designing therapeutic inhibitors. For example, ADAMTS5, a major drug target in arthritis, is activated extracellularly, making itself and its activators, furin, PC7, and PACE4 (6, 35), attractive targets for drugs that do not cross the cell membrane. The involvement of ADAMTS15 activity in arthritis is not yet explored, although its mRNA is present and regulated in a similar manner to that of ADAMTS5 in osteoarthritis (36), and aggrecan has been previously reported as its substrate (33).

Common to all ADAMTS proteoglycanases described to date is their propeptide processing by furin activity and their ability to cleave the versican VI splice variant at the $E^{441} \downarrow A^{442}$ site generating the neoepitope DPEAAE. This study shows that ADAMTS15 is no exception. An intriguing finding in this study, however, was the ability of the catalytic domain of ADAMTS15 alone to also cleave versican. This suggests that sites on the ADAMTS15 catalytic domain can mediate substrate binding as also indicated in this study by its heparin sensitivity. This is in stark contrast to other ADAMTS proteoglycanases described to date, for example ADAMTS5 ProCat activity against aggrecan (37). Although we did not observe apparent autocatalysis in our study using an E362A mutant (data not shown), other ADAMTS proteoglycanases have been reported to undergo this process (38), and the difficulty in detecting the mature form of full-length ADAMTS15 in this study suggests it to be relatively unstable. The one implication of C-terminal processing is the removal of substrate-binding sites found in the ancillary domain (37–39), essentially inactivating the protease.

Substrate-binding sites in ADAMTS ancillary domains (exosites) have become regions of interest because competitive inhibitors could theoretically be designed against those sites. Therefore, determining their role in ECM binding is important. In our study, we could not efficiently detect full-length active ADAMTS15 in the conditioned medium without the addition of heparin. Thus, it is possible that full-length ADAMTS15 is tightly bound to the cell surface and ECM, as further confirmed in this study by *in vitro* cell-surface biotinylation and co-localization with hyaluronan within tissues, including skeletal muscle in the developing mouse hind limb, via specific ECM-binding sites yet to be identified. Of the ADAMTS proteoglycanases, ADAMTS1, -4, and -9 are known to be localized to the cell surface (5, 9, 40), in contrast to ADAMTS5, which is present in the pericellular matrix but not found on the cell surface (6, 41).

Because nothing was known about the expression of *Adamts15* during embryonic development, we characterized its expression across key developmental time points that have been well described for other *Adamts* proteoglycanases and

their substrate versican. *Adamts15* was expressed in sites overlapping with versican, particularly during early heart development. Versican knock-out mice (*hdf*) die of a heart defect at E10.5 dpc (42), whereas *Adamts5* knock-out mice and *Adamts9* heterozygote mice hearts present with myxomatous heart valves and chondrogenic nodules, respectively (18, 43). Given the strong and specific expression of *Adamts15* in the E10.5 dpc mouse embryonic heart, it is attractive to hypothesize a role for ADAMTS15 during heart development through versican processing. Later in development, at E13.5 dpc, *Adamts15* was expressed in the perichondrium of the developing autopod, where *Adamts1*, *-5*, *-9,* and *-20* and versican (*Cspg2*) are all expressed and cooperate to stimulate interdigital apoptosis to form pentameric digits (17, 31, 44). Therefore, *Adamts15* might also participate in this process. Interestingly, *Adamts15* was also widely expressed in the hind limb of E15.5 embryos, including condensing cartilage of the long bones, a site overlapping with *Adamts9* expression (31). At this stage of development, versican provides a transitional matrix that is cleared upon aggrecan deposition to form immature cartilage (45). A role for the ADAMTS proteoglycanases during this process has not yet been clearly defined, but both ADAMTS9 and ADAMTS15 are likely candidates.

In this study, we showed ADAMTS15 expression in skeletal muscle of the developing mouse hind limb. This is in accordance with our recent study showing that ADAMTS15 could rescue an *Adamts5*-deficient myoblast fusion defect in an *in vitro* model of skeletal muscle fiber formation, mouse C2C12 cells (46). This study highlighted the expansion of a versican and hyaluronan-rich pericellular matrix surrounding myoblasts upon *Adamts5* silencing, leading to the hypothesis that ADAMTS15 cooperates with ADAMTS5 to clear the pericellular matrix surrounding myoblasts during *in vivo* myogenesis, thus facilitating myoblast fusion and mature skeletal muscle fiber formation.

Given the association between *ADAMTS15* and colorectal cancer described above, we supposed that *Adamts15* could be expressed in the adult mouse colon. Immunostaining with an ADAMTS15 antibody directed toward its prodomain robustly detected ADAMTS15 in several areas of the large intestine, including the muscular externa, submucosa and submucosal glands, crypts, and villi. The function of ADAMTS15 in the colon is not known; however, its broad and high expression level is concordant with its proposed role in colorectal cancer as a tumor suppressor gene. Although the mechanism(s) underlying ADAMTS15's tumor suppression capabilities are unknown, the anti-angiogenic nature of several other ADAMTS proteoglycanases has been characterized, including ADAMTS15's evolutionary partner ADAMTS8 (47–50). In addition, ADAMTS9 has recently been identified as a putative tumor suppressor gene through its anti-angiogenic properties in esophageal and nasopharyngeal carcinoma (51).

This study highlights the similarities and differences in the activation, substrate specificity, and expression of ADAMTS15 compared with other ADAMTS proteoglycanase family members. We have characterized ADAMTS15 as a novel versicanase that is present in biological tissues during embryogenesis relevant to versican biology. Our data provide a solid justification for further investigation of the function of ADAMTS15 during embryonic heart and musculoskeletal development, and it gives further insights into its mechanism of action that might be relevant in pathologies such as arthritis and cancer.

Acknowledgment—We thank Prof. Suneel Apte for critical evaluation of the manuscript and valuable intellectual input throughout the study.

REFERENCES

1. Apte, S. S. (2009) A disintegrin-like and metalloprotease (reprolysin-type) with thrombospondin type 1 motif (ADAMTS) superfamily: functions and mechanisms. *J. Biol. Chem.* **284,** 31493–31497
2. Tsai, H. M. (2002) Deficiency of ADAMTS13 in thrombotic thrombocytopenic purpura. *Int. J. Hematol.* **76,** 132–138
3. Dagoneau, N., Benoist-Lasselin, C., Huber, C., Faivre, L., Mégarbané, A., Alswaid, A., Dollfus, H., Alembik, Y., Munnich, A., Legeai-Mallet, L., and Cormier-Daire, V. (2004) ADAMTS10 mutations in autosomal recessive Weill-Marchesani syndrome. *Am. J. Hum. Genet.* **75,** 801–806
4. Colige, A., Nuytinck, L., Hausser, I., van Essen, A. J., Thiry, M., Herens, C., Adès, L. C., Malfait, F., Paepe, A. D., Franck, P., Wolff, G., Oosterwijk, J. C., Smitt, J. H., Lapière, C. M., and Nusgens, B. V. (2004) Novel types of mutation responsible for the dermatosparactic type of Ehlers-Danlos syndrome (type VIIC) and common polymorphisms in the ADAMTS2 gene. *J. Invest. Dermatol.* **123,** 656–663
5. Koo, B. H., Longpré, J. M., Somerville, R. P., Alexander, J. P., Leduc, R., and Apte, S. S. (2006) Cell-surface processing of pro-ADAMTS9 by furin. *J. Biol. Chem.* **281,** 12485–12494
6. Longpré, J. M., McCulloch, D. R., Koo, B. H., Alexander, J. P., Apte, S. S., and Leduc, R. (2009) Characterization of proADAMTS5 processing by proprotein convertases. *Int. J. Biochem. Cell Biol.* **41,** 1116–1126
7. Sandy, J. D., Westling, J., Kenagy, R. D., Iruela-Arispe, M. L., Verscharen, C., Rodriguez-Mazaneque, J. C., Zimmermann, D. R., Lemire, J. M., Fischer, J. W., Wight, T. N., and Clowes, A. W. (2001) Versican V1 proteolysis in human aorta *in vivo* occurs at the Glu^{441}–Ala^{442} bond, a site that is cleaved by recombinant ADAMTS-1 and ADAMTS-4. *J. Biol. Chem.* **276,** 13372–13378
8. Gao, G., Plaas, A., Thompson, V. P., Jin, S., Zuo, F., and Sandy, J. D. (2004) ADAMTS4 (aggrecanase-1) activation on the cell surface involves C-terminal cleavage by glycosylphosphatidylinositol-anchored membrane type 4-matrix metalloproteinase and binding of the activated proteinase to chondroitin sulfate and heparan sulfate on syndecan-1. *J. Biol. Chem.* **279,** 10042–10051
9. Longpré, J. M., and Leduc, R. (2004) Identification of prodomain determinants involved in ADAMTS-1 biosynthesis. *J. Biol. Chem.* **279,** 33237–33245
10. Wang, P., Tortorella, M., England, K., Malfait, A. M., Thomas, G., Arner, E. C., and Pei, D. (2004) Proprotein convertase furin interacts with and cleaves pro-ADAMTS4 (Aggrecanase-1) in the trans-Golgi network. *J. Biol. Chem.* **279,** 15434–15440
11. Westling, J., Fosang, A. J., Last, K., Thompson, V. P., Tomkinson, K. N., Hebert, T., McDonagh, T., Collins-Racie, L. A., LaVallie, E. R., Morris, E. A., and Sandy, J. D. (2002) ADAMTS4 cleaves at the aggrecanase site (Glu^{373}–Ala^{374}) and secondarily at the matrix metalloproteinase site (Asn^{341}–Phe^{342}) in the aggrecan interglobular domain. *J. Biol. Chem.* **277,** 16059–16066
12. Koo, B. H., Longpré, J. M., Somerville, R. P., Alexander, J. P., Leduc, R., and Apte, S. S. (2007) Regulation of ADAMTS9 secretion and enzymatic activity by its propeptide. *J. Biol. Chem.* **282,** 16146–16154
13. Russell, D. L., Doyle, K. M., Ochsner, S. A., Sandy, J. D., and Richards, J. S. (2003) Processing and localization of ADAMTS-1 and proteolytic cleavage of versican during cumulus matrix expansion and ovulation. *J. Biol. Chem.* **278,** 42330–42339
14. Yokoyama, H., Wada, T., Kobayashi, K., Kuno, K., Kurihara, H., Shindo, T., and Matsushima, K. (2002) A disintegrin and metalloproteinase with

thrombospondin motifs (ADAMTS)-1 null mutant mice develop renal lesions mimicking obstructive nephropathy. *Nephrol. Dial. Transplant.* **17,** 39–41
15. Enomoto, H., Nelson, C. M., Somerville, R. P., Mielke, K., Dixon, L. J., Powell, K., and Apte, S. S. (2010) Cooperation of two ADAMTS metalloproteases in closure of the mouse palate identifies a requirement for versican proteolysis in regulating palatal mesenchyme proliferation. *Development* **137,** 4029–4038
16. Silver, D. L., Hou, L., Somerville, R., Young, M. E., Apte, S. S., and Pavan, W. J. (2008) The secreted metalloprotease ADAMTS20 is required for melanoblast survival. *PLoS Genet.* **4,** e1000003
17. McCulloch, D. R., Nelson, C. M., Dixon, L. J., Silver, D. L., Wylie, J. D., Lindner, V., Sasaki, T., Cooley, M. A., Argraves, W. S., and Apte, S. S. (2009) ADAMTS metalloproteases generate active versican fragments that regulate interdigital web regression. *Dev. Cell* **17,** 687–698
18. Dupuis, L. E., McCulloch, D. R., McGarity, J. D., Bahan, A., Wessels, A., Weber, D., Diminich, A. M., Nelson, C. M., Apte, S. S., and Kern, C. B. (2011) Altered versican cleavage in ADAMTS5-deficient mice; a novel etiology of myxomatous valve disease. *Dev. Biol.* **357,** 152–164
19. Dupuis, L. E., Osinska, H., Weinstein, M. B., Hinton, R. B., and Kern, C. B. (2013) Insufficient versican cleavage and Smad2 phosphorylation results in bicuspid aortic and pulmonary valves. *J. Mol. Cell. Cardiol.* **60,** 50–59
20. Glasson, S. S., Askew, R., Sheppard, B., Carito, B., Blanchet, T., Ma, H. L., Flannery, C. R., Peluso, D., Kanki, K., Yang, Z., Majumdar, M. K., and Morris, E. A. (2005) Deletion of active ADAMTS5 prevents cartilage degradation in a murine model of osteoarthritis. *Nature* **434,** 644–648
21. Stanton, H., Rogerson, F. M., East, C. J., Golub, S. B., Lawlor, K. E., Meeker, C. T., Little, C. B., Last, K., Farmer, P. J., Campbell, I. K., Fourie, A. M., and Fosang, A. J. (2005) ADAMTS5 is the major aggrecanase in mouse cartilage *in vivo* and *in vitro*. *Nature* **434,** 648–652
22. Porter, S., Span, P. N., Sweep, F. C., Tjan-Heijnen, V. C., Pennington, C. J., Pedersen, T. X., Johnsen, M., Lund, L. R., Rømer, J., and Edwards, D. R. (2006) ADAMTS8 and ADAMTS15 expression predicts survival in human breast carcinoma. *Int. J. Cancer* **118,** 1241–1247
23. Viloria, C. G., Obaya, A. J., Moncada-Pazos, A., Llamazares, M., Astudillo, A., Capellá, G., Cal, S., and López-Otín, C. (2009) Genetic inactivation of ADAMTS15 metalloprotease in human colorectal cancer. *Cancer Res.* **69,** 4926–4934
24. Cross, N. A., Chandrasekharan, S., Jokonya, N., Fowles, A., Hamdy, F. C., Buttle, D. J., and Eaton, C. L. (2005) The expression and regulation of ADAMTS-1, -4, -5, -9, and -15, and TIMP-3 by TGFβ1 in prostate cells: relevance to the accumulation of versican. *Prostate* **63,** 269–275
25. Molokwu, C. N., Adeniji, O. O., Chandrasekharan, S., Hamdy, F. C., and Buttle, D. J. (2010) Androgen regulates ADAMTS15 gene expression in prostate cancer cells. *Cancer Invest.* **28,** 698–710
26. Kischel, P., Waltregny, D., Dumont, B., Turtoi, A., Greffe, Y., Kirsch, S., De Pauw, E., and Castronovo, V. (2010) Versican overexpression in human breast cancer lesions: known and new isoforms for stromal tumor targeting. *Int. J. Cancer* **126,** 640–650
27. Ricciardelli, C., Russell, D. L., Ween, M. P., Mayne, K., Suwiwat, S., Byers, S., Marshall, V. R., Tilley, W. D., and Horsfall, D. J. (2007) Formation of hyaluronan- and versican-rich pericellular matrix by prostate cancer cells promotes cell motility. *J. Biol. Chem.* **282,** 10814–10825
28. Ween, M. P., Hummitzsch, K., Rodgers, R. J., Oehler, M. K., and Ricciardelli, C. (2011) Versican induces a pro-metastatic ovarian cancer cell behavior which can be inhibited by small hyaluronan oligosaccharides. *Clin. Exp. Metastasis* **28,** 113–125
29. McCulloch, D. R., Wylie, J. D., Longpre, J. M., Leduc, R., and Apte, S. S. (2010) 10 mM glucosamine prevents activation of proADAMTS5 (aggrecanase-2) in transfected cells by interference with post-translational modification of furin. *Osteoarthritis Cartilage* **18,** 455–463
30. Yamaji, R., Chatani, E., Harada, N., Sugimoto, K., Inui, H., and Nakano, Y. (2005) Glyceraldehyde-3-phosphate dehydrogenase in the extracellular space inhibits cell spreading. *Biochim. Biophys. Acta* **1726,** 261–271
31. Jungers, K. A., Le Goff, C., Somerville, R. P., and Apte, S. S. (2005) Adamts9 is widely expressed during mouse embryo development. *Gene Expr. Patterns* **5,** 609–617
32. McCulloch, D. R., Le Goff, C., Bhatt, S., Dixon, L. J., Sandy, J. D., and Apte, S. S. (2009) Adamts5, the gene encoding a proteoglycan-degrading metalloprotease, is expressed by specific cell lineages during mouse embryonic development and in adult tissues. *Gene Expr. Patterns* **9,** 314–323
33. Kintakas, C., and McCulloch, D. R. (2011) Emerging roles for ADAMTS5 during development and disease. *Matrix Biol.* **30,** 311–317
34. Rodríguez-Manzaneque, J. C., Westling, J., Thai, S. N., Luque, A., Knauper, V., Murphy, G., Sandy, J. D., and Iruela-Arispe, M. L. (2002) ADAMTS1 cleaves aggrecan at multiple sites and is differentially inhibited by metalloproteinase inhibitors. *Biochem. Biophys. Res. Commun.* **293,** 501–508
35. Malfait, A. M., Arner, E. C., Song, R. H., Alston, J. T., Markosyan, S., Staten, N., Yang, Z., Griggs, D. W., and Tortorella, M. D. (2008) Proprotein convertase activation of aggrecanases in cartilage *in situ*. *Arch. Biochem. Biophys.* **478,** 43–51
36. Kevorkian, L., Young, D. A., Darrah, C., Donell, S. T., Shepstone, L., Porter, S., Brockbank, S. M., Edwards, D. R., Parker, A. E., and Clark, I. M. (2004) Expression profiling of metalloproteinases and their inhibitors in cartilage. *Arthritis Rheum.* **50,** 131–141
37. Gendron, C., Kashiwagi, M., Lim, N. H., Enghild, J. J., Thøgersen, I. B., Hughes, C., Caterson, B., and Nagase, H. (2007) Proteolytic activities of human ADAMTS-5: comparative studies with ADAMTS-4. *J. Biol. Chem.* **282,** 18294–18306
38. Zeng, W., Corcoran, C., Collins-Racie, L. A., Lavallie, E. R., Morris, E. A., and Flannery, C. R. (2006) Glycosaminoglycan-binding properties and aggrecanase activities of truncated ADAMTSs: comparative analyses with ADAMTS-5, -9, -16, and -18. *Biochim. Biophys. Acta* **1760,** 517–524
39. Fushimi, K., Troeberg, L., Nakamura, H., Lim, N. H., and Nagase, H. (2008) Functional differences of the catalytic and non-catalytic domains in human ADAMTS-4 and ADAMTS-5 in aggrecanolytic activity. *J. Biol. Chem.* **283,** 6706–6716
40. Mayer, G., Hamelin, J., Asselin, M. C., Pasquato, A., Marcinkiewicz, E., Tang, M., Tabibzadeh, S., and Seidah, N. G. (2008) The regulated cell surface zymogen activation of the proprotein convertase PC5A directs the processing of its secretory substrates. *J. Biol. Chem.* **283,** 2373–2384
41. Plaas, A., Osborn, B., Yoshihara, Y., Bai, Y., Bloom, T., Nelson, F., Mikecz, K., and Sandy, J. D. (2007) Aggrecanolysis in human osteoarthritis: confocal localization and biochemical characterization of ADAMTS5-hyaluronan complexes in articular cartilages. *Osteoarthritis Cartilage* **15,** 719–734
42. Mjaatvedt, C. H., Yamamura, H., Capehart, A. A., Turner, D., and Markwald, R. R. (1998) The Cspg2 gene, disrupted in the hdf mutant, is required for right cardiac chamber and endocardial cushion formation. *Dev. Biol.* **202,** 56–66
43. Kern, C. B., Wessels, A., McGarity, J., Dixon, L. J., Alston, E., Argraves, W. S., Geeting, D., Nelson, C. M., Menick, D. R., and Apte, S. S. (2010) Reduced versican cleavage due to Adamts9 haploinsufficiency is associated with cardiac and aortic anomalies. *Matrix Biol.* **29,** 304–316
44. Thai, S. N., and Iruela-Arispe, M. L. (2002) Expression of ADAMTS1 during murine development. *Mech. Dev.* **115,** 181–185
45. Snow, H. E., Riccio, L. M., Mjaatvedt, C. H., Hoffman, S., and Capehart, A. A. (2005) Versican expression during skeletal/joint morphogenesis and patterning of muscle and nerve in the embryonic mouse limb. *Anat. Rec. A Discov. Mol. Cell. Evol. Biol.* **282,** 95–105
46. Stupka, N., Kintakas, C., White, J. D., Fraser, F. W., Hanciu, M., Aramaki-Hattori, N., Martin, S., Coles, C., Collier, F., Ward, A. C., Apte, S. S., and McCulloch, D. R. (2013) Versican processing by a disintegrin-like and metalloproteinase domain with thrombospondin-1 repeats proteinases-5 and -15 facilitates myoblast fusion. *J. Biol. Chem.* **288,** 1907–1917
47. Dunn, J. R., Reed, J. E., du Plessis, D. G., Shaw, E. J., Reeves, P., Gee, A. L., Warnke, P., and Walker, C. (2006) Expression of ADAMTS-8, a secreted protease with antiangiogenic properties, is downregulated in brain tumours. *Br. J. Cancer* **94,** 1186–1193
48. Hsu, Y. P., Staton, C. A., Cross, N., and Buttle, D. J. (2012) Anti-angiogenic properties of ADAMTS-4 *in vitro*. *Int. J. Exp. Pathol.* **93,** 70–77
49. Koo, B. H., Coe, D. M., Dixon, L. J., Somerville, R. P., Nelson, C. M., Wang,

L. W., Young, M. E., Lindner, D. J., and Apte, S. S. (2010) ADAMTS9 is a cell-autonomously acting, anti-angiogenic metalloprotease expressed by microvascular endothelial cells. *Am. J. Pathol.* **176,** 1494–1504

50. Liu, Y. J., Xu, Y., and Yu, Q. (2006) Full-length ADAMTS-1 and the ADAMTS-1 fragments display pro- and antimetastatic activity, respectively. *Oncogene* **25,** 2452–2467
51. Lo, P. H., Lung, H. L., Cheung, A. K., Apte, S. S., Chan, K. W., Kwong, F. M., Ko, J. M., Cheng, Y., Law, S., Srivastava, G., Zabarovsky, E. R., Tsao, S. W., Tang, J. C., Stanbridge, E. J., and Lung, M. L. (2010) Extracellular protease ADAMTS9 suppresses esophageal and nasopharyngeal carcinoma tumor formation by inhibiting angiogenesis. *Cancer Res.* **70,** 5567–5576